RSC Advances

This is an *Accepted Manuscript*, which has been through the Royal Society of Chemistry peer review process and has been accepted for publication.

Accepted Manuscripts are published online shortly after acceptance, before technical editing, formatting and proof reading. Using this free service, authors can make their results available to the community, in citable form, before we publish the edited article. This *Accepted Manuscript* will be replaced by the edited, formatted and paginated article as soon as this is available.

You can find more information about *Accepted Manuscripts* in the **Information for Authors**.

ROYAL SOCIETY OF CHEMISTRY

www.rsc.org/advances

RSC Advances

ARTICLE

A theoretical approach to understand the inhibition mechanism of steel corrosion by the two aminobenzonitrile inhibitors

Sourav Kr. Saha [a,b] and Priyabrata Banerjee [a,b]*

In this work, the adsorption behavior and corresponding inhibition mechanism of two aminobenzonitrile derivatives *e.g;* 2-aminobenzonitrile (2-AB) and 3-aminobenzonitrile (3-AB) in aqueous acidic medium on the steel surfaces have been investigated by the quantum chemical calculation and molecular dynamics (MD) simulation method. Quantum chemical parameters such as E_{HOMO}, E_{LUMO}, energy gaps (ΔE), dipole moment (μ), global hardness (η), softness (S), fraction of electron transfer from the inhibitors molecule to the metallic surface (ΔN) have been calculated and well discussed. Fukui indices analysis are performed in getting local reactive sites of the studied inhibitor molecules. Furthermore, molecular dynamics simulation is applied to search the best adorable adsorption configuration of inhibitor over iron (1 1 0) surface.

1. Introduction

Nowadays prevention of metallic corrosion is an important issue considering enormous role of metals and its alloys in several industrial applications. Iron and its alloys use to play crucial roles in almost all mechanical industries.[1-3] In several industrial process uses of an acid solution in several numerous techniques such as acid cleaning, acid pickling, acid descaling are very common.[4,5] These acid solutions create serious metallic corrosion on the metallic surfaces. Due to this adverse impact on metallic bodies, now a days almost all the industries are suffering from a huge and incredible amount of economic losses. Therefore, prevention of corrosion is an urgently needed thing and our prima facie interest is to protect this kind of solution state metallic corrosion. Among the numerous corrosion inhibition techniques, uses of inhibitors have been widely acceptable technique due to its low cost, high efficiency and facile-feasibility.[6,7] In general, organic compounds having heteroatoms with lone pair of electrons (N, O, S and P), aromatic rings, π conjugated systems, conjugated aliphatic bonds are considered to be effective corrosion inhibitors.[8-10] Such organic inhibitors adhere on the metallic surface by the physical adsorption (electrostatic interactions) or chemical adsorption (coordination bond) route and thereby can protect metallic corrosion. In physical adsorption, inhibitors molecules adsorbed on the metallic surface by the electrostatic interactions between the charged inhibitor molecules and charged metallic surfaces.[11,12] In chemical adsorption inhibitor molecules donate its electron to the vacant d-orbitals of metals for the sake of forming a coordinate bond and have possibility to accept electrons from the metallic surface by using their antibonding orbitals to form a backbond.[13] These two adsorption process produces a uniform film on the metallic surface, which in turn prevent the metallic surface from the aggressive acid attacks. However, in detail description of this surface phenomenon and factors determining the strength of interaction is yet to be explored. In this present investigation we have tried to explain how this process occurs and the contributing factors in controlling the adsorption process.

Traditionally, performance of inhibitive action is found out by the weight loss measurements, potentiodynamic polarization and electrochemical impedance spectroscopy. However, these experimental methodologies are costly, time consuming and sometimes unable to explore inhibition mechanisms.[14,15] With the improvement of sophisticated software and hardware related computational supportive systems, computer aided simulation has been explored as an easy and power full tool from where we can investigate the complex system in corrosion process and may successfully predict their relative inhibition efficiency well in advance. In this occasion proper theoretical modeling and corresponding quantum chemical calculation is very efficient for exploring the relationship between the molecular properties of the inhibitors and its corrosion inhibition efficiencies.[16-20] Corrosion inhibition capability of the molecules can be determined by the frontier molecular orbital energies, energy gap, dipolemoment, global hardness, softness, fraction of electron transfer from the inhibitors molecule to the metallic surface *etc*. In our previous works, we have successfully investigated the correlation between the quantum chemical calculations and experimentally obtained corrosion inhibition effectiveness of the pyrazine derivatives [21], mercapto-quinoline derivatives [22] and Schiff base [23] molecules. However, Kokalj *et al* recently proposed that only quantum chemical approach is not sufficient enough to envisage the inhibition efficiency trend of the inhibitors molecules.[24,25] In many cases, results obtained from DFT cannot be correlated well with obtained experimental findings.[26,27] In this circumstances, a precise modelling of experimentation should be emphasized to correlate the theoretical results with the experimental inhibition effectiveness. In real practice, modeling of experiment can only provide the actual interfacial interactions between the concerned metallic surface and inhibitor molecules. As a result, recently molecular dynamics (MD) simulation has been immerged as a modern tool from where we can reasonably predict actual interfacial configuration and adsorption energies of the surface adsorbed inhibitor molecules. Till date only a few certain groups are working on it to get the interaction as well as binding energy of surface adsorbed inhibitor molecules. Obot *et al*, recently has employed MD simulation to study the adsorption behaviour of pyrazine derivatives on the steel surface.[28] Xia *et al*,

explored the correlation between the structural conformation of the imidazoline derivatives and their corresponding inhibition efficiencies by employing MD.[29]

In this present investigation, we have successfully studied both the quantum chemical calculation and MD simulations to explore the correlation between the theoretical results and previously obtained experimental findings. The aim of this present work is to find out an alternative approach from where we can predict which molecules will behave as a good corrosion inhibitors and which will not. This is obviously of certain importance with respect to the economic point of view. In view of above, in our present work quantum chemical calculation and MD simulation have been carried out on some recently studied inhibitor molecules namely, 2-aminobenzonitrile, 3-aminobenzonitrile over the steel surface in the acidic media.[30] The results obtained from these theoretical studies are in well accordance with the results obtained from the experimental outcomes.

2. Computational details

2.1. Quantum chemical calculation

Density functional theory (DFT) is a worldwide accepted *ab initio* approach for modelling ground state properties of molecules of interest. In last few decades, DFT has become popular due to its accuracy in carrying out theoretical calculation in lesser time with a much lesser amount of investment. In this present work, quantum chemical calculations were carried out with ORCA program module version 2.7.0, which is an open source code developed by Prof. Dr. Frank Neese (Director, MPI für Chemische Energiekonversion, Muelheim, Germany).[31] Geometry optimizations of the presently studied inhibitor molecules were performed using hybrid B3LYP functional.[32-37] The all-electron Gaussian basis sets are developed by Ahlrichs group.[38] In this study, triple-ζ quality basis sets TZV(P) along with one set of polarization function on the N heteroatom was used.[39] For carbon and hydrogen like atoms relatively smaller polarized split-valence SV(P) basis sets are used which is of double-ζ quality in the valence region and had a polarizing set of d functions on the non hydrogen atoms. Self consistent field (SCF) calculations were converged [with 10^{-7} Eh: density change, 10^{-8} Eh: energy, 10^{-7}: maximum element of the DIIS (Direct Inversion in the Iterative Subspace or Direct Inversion of the Iterative Subspace) error vector]. As electrochemical corrosion always happen in aqueous phase it is necessary to use the effect of solvent in all the DFT calculations. Therefore in this present study effect of solvent is included for the sake of clarity. Here, COSMO model was applied in order to incorporate the effect of solvent (water) in this calculation. This method is used for modelling of water as a continuum of uniform dielectric constant (ε) and the solute was placed as a uniform series of inlocking atomic spheres.

Local reactivity of the molecule has been analyzed by evaluation of Fukui indices (FI). The FI calculation are performed using Dmol^3 module, Material studio^{TM} version 6.1 by Accelrys Inc, San Diego, CA.[40] All the calculations are accomplished using the double numerical polarization (DNP) basis set (including d as well as p orbital polarization functional) along with generalized gradient approximation and BLYP exchange-correlation functionals.[41,42] Detail information of local reactivity has been obtained by condensed Fukui functions.[43] Herein, Fukui function (f_k) can be expressed as first derivative of the electronic density w.r.t the number of electrons (N) in a constant external potential.[44]

$$f_k = \left(\frac{\partial \rho(\vec{r})}{\partial N} \right)_{\upsilon(\vec{r})} \tag{1}$$

For electron transfer reaction, Fukui functions enlighten the sites in a molecule where nucleophilic, electrophilic or radical attack are mostly possible. The Fukui functions are calculated by taking the finite difference approximations as:[45]

$$f_k^+ = q_k(N+1) - q_k(N) \quad \text{(for nucleophilic attack)} \tag{2}$$

$$f_k^- = q_k(N) - q_k(N-1) \quad \text{(for electrophilic attack)} \tag{3}$$

where q_k is the gross charge of k atom *i.e.;* the electronic density at a particular point (r) in space around the concerned molecule. The q_k (N+1), q_k (N) and q_k (N-1) are defined as the charge of the anionic, neutral and cationic species respectively. Hirshfeld population analysis (HPA) is used for the presentation of Fukui functions.[46]

2.2. Molecular Dynamics simulation

Adsorption process of the aminobenzonitrile compounds on the iron surface is investigated by MD simulation using Material Studio^{TM} software 6.1 (from Accelrys Inc.).[40] In this present investigation, we have chosen Fe (1 1 0) surface for simulation. In this simulation process interaction between the studied molecules and iron surface are carried out in a simulation box of (39.47× 39.47 × 77.23 Å) with periodic boundary condition in order to avoid any arbitrary boundary effects. Here, we have used ten layers of iron atoms as it provides sufficient depth to overcome the issue related to cutoff radius in this case. In this investigation, simulation box is created by a three layer. The first layer contain Fe slab and the second layer is the solution slab which contains H_2O, H_3O^+, Cl^- molecules as well as molecular ions and the remaining part of the box is the vacuum layer. After construction of the simulation box, molecular dynamic simulation is carried out using the COMPASS (Condensed Phase Optimized Molecular Potentials for Atomistic Simulation Studies) force field. COMPASS is a highly accepted and authentic ab initio force field that enables accurate prediction of nature for a good many number of chemical entities. In general, the parameterization procedure can be divided in two phases: (i) ab initio parameterization, (ii) empirical optimization.[47] The MD simulations are performed both at 298.0 K and 328.0 K using canonical ensemble (NVT) with a time step of 1.0 fs and a simulation time of 500 ps.

The interaction energy ($E_{interaction}$) and binding energy ($E_{binding}$) of the inhibitor molecule on the Fe (1 1 0) surface are obtained by the following eqn (4) and (5).[40]

$$E_{interaction} = E_{total} - (E_{surface + H_2O + H_3O^+ + Cl^-} + E_{inhibitor}) \tag{4}$$

Where E_{total} is the total energy of the simulation system, $E_{surface+H2O+H3O^+ + Cl^-}$ is the energy of the iron surface together with H_2O, H_3O^+, Cl^- molecule, ions and $E_{inhibitor}$ is the energy of the free inhibitor molecule.

The binding energy of the inhibitor molecule is negative value of interaction energy is as follows [23]

$$E_{binding} = -E_{interaction} \tag{5}$$

3. Results and discussion
3.1. Comparative experimental studies between two studied inhibitors

G. Sığırcık *et al* have recently investigated corrosion inhibition effectiveness of aminobenzonitrile compounds (Fig. 1) on the steel surface in 0.5 M HCl solution by the complete wet chemical
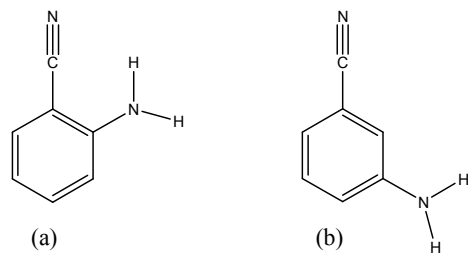
Fig. 1 Chemical structure of studied corrosion inhibitors: (a) 2-aminobenzonitrile (2-AB) and (b) 3-aminobenzonitrile (3-AB).

experimentation.[30] The obtained experimental results have reflected that these two inhibitors are remarkably good corrosion resistant inhibitors in 0.5 M HCl medium. The order of inhibition efficiency obtained from potentiodynamic polarization as well as electrochemical impedance spectroscopy measurements follows the order: 3-AB > 2-AB. In quest of finding out the probable reason for relative inhibition order of these two inhibitors, it was found that authors are only pointing that steric effect between the two adjacent group (-NH$_2$ and -C≡N) plays the crucial role. Authors have stated that the steric effect in 2-AB is comparatively higher than that of 3-AB. For this reason, 3-AB is adsorbing comparatively in a better way than that of 2-AB and higher inhibition efficiency is obtained.

These authors felt that the explanation is not well and sufficient enough in order to explain this relative order of inhibition efficiency. In getting a complete picture of the mechanism of inhibition action of the two aminobenzonitrile compounds as well as to get explanation of this inhibition efficiency trend, quantum chemical calculation and MD simulation are carried out in this present investigation. In addition, correlations among the observed molecular parameters and experimentally obtained inhibition efficiency outcomes have also been performed.

3.2. Quantum chemical calculations of neutral form of inhibitor molecules

3.2.1. Equilibrium geometry structure

The optimized geometric configurations of the molecules (2-AB and 3-AB) are shown in Fig. 2 and their bond angle, bond lengths are presented in Table 1. It can be seen from Table 1, that all the C-C bond length of the benzene ring are lying in the range of 1.388Å - 1.427Å. Thus, C-C bond length in the benzene ring are longer than the general C=C double bonds and shorter than the C-C single bonds.[48] The tendency of intermediate bond lengths obviously indicate presence of a conjugation effect in the benzene ring.

From Table 1, it could be seen that the bond angles of benzene rings in 2-AB and 3-AB molecules are lying in the range of 118° to 121.5° means atoms in 2-AB and 3-AB molecules are all sp^2 hybridized. Therefore, from bond length and bond angle values it can be concluded that both the optimized structure of the inhibitor molecule possessed ideal geometric configuration.

3.2.2. Frontier orbitals energies

Highest occupied molecular orbital (E_{HOMO}) and lowest unoccupied molecular orbital (E_{LUMO}) are very useful to elucidate chemical reactivity of a molecule. According to the frontier molecular orbital theory of chemical reactivity, transition of electrons mainly related to the highest occupied molecular orbital (HOMO) and lowest unoccupied molecular orbital (LUMO) of the reacting species.[49] HOMO is associated to the electron donation capability of the molecule. Higher the E_{HOMO} value, stronger will

Table 1 Bond length (Å) and bond angle (°) of the optimized neutral form of inhibitor molecules

Geometry parameters	2-AB	3-AB
Bond length		
C1—C2	1.4279	1.4054
C2—C3	1.4144	1.4085
C3—C4	1.3882	1.3985
C4—C5	1.4088	1.3946
C5—C6	1.3890	1.4161
Bond angle		
C1—C2—C3	120.67	121.48
C2—C3—C4	120.69	118.07
C3—C4—C5	118.89	121.19
C4—C5—C6	121.34	121.00
C5—C6—C1	121.00	118.16

be the electron donating capability of inhibitor and therefore better the inhibition efficiency will be observed.[50] LUMO imply the capability of the molecules to accept electrons from the metallic surface. Lower the value of E_{LUMO}, more it will be prone towards accepting electrons.[51] From, Table 2 it can be seen that E_{HOMO} value increased in the order of 2-AB < 3-AB, that means ability to donate electron from the inhibitor molecule to the metallic surface obeys the order 3-AB > 2-AB. The calculated E_{LUMO} value exemplifies that the electron acceptance capability decreased in the order of 3-AB > 2-AB. Hence, the orders (E_{HOMO} and E_{LUMO}) are correlated strongly with experimental inhibition efficiencies.

Apart from E_{HOMO} and E_{LUMO}, energy gap (ΔE) is also an important parameter in determining adsorption of organic molecule on the metallic surface. As ΔE decreased, reactivity of the molecule will definitely increase, which in turn leading to an increase in adsorption onto a metallic surface.[52] In general, molecule with comparatively lower energy gap is better polarizable and in turn associated with higher chemical reactivity and lower kinetic stability. In this connection, ΔE has been used to elucidate binding ability of the inhibitor molecule on the metallic surface. It can be seen (*vide* Table 2), that the ΔE value follows the trend 2-AB > 3-AB, which is again also well in accordance with the result obtained from the experimental outcomes. Dipolemoment (μ) of a molecule is also an important parameter to elucidate chemical reactivity of a molecule. A literature survey reveals that adsorption process is more facilitated with increasing values of dipolemoment as it is influencing the transport process through the adsorbed layer.[53,54] In this work it can be observed from Table 2 that dipolemoment values are increased in the order of 2-AB < 3-AB, which further more strengthen the experimental results.

According to the Koopmans' theorem, E_{HOMO} and E_{LUMO} of the inhibitor molecule are related to the ionization potential (I) and electron affinity (A) by the following equations:[55]

$$I = -E_{HOMO} \qquad (6)$$

$$A = -E_{LUMO} \qquad (7)$$

Electronegativity (χ) and global hardness (η) of the concerned inhibitor molecules are obtained from the ionization potential and electron affinity values. By the following formula these parameters are related to ionization potential and electron affinity:

$$\chi = \frac{I + A}{2} \qquad (8)$$

Table 2 Calculated quantum chemical parameters of the studied inhibitors in neutral form

Inhibitors	E_{HOMO} (eV)	E_{LUMO} (eV)	ΔE (eV)	μ (Debye)	$I = -E_{HOMO}$	$A = -E_{LUMO}$	χ (eV)	η (eV)	σ (eV^{-1})	ΔN_{100}	ΔN_{110}	ΔN_{111}	Inhibition efficiency[a]
2-AB	-5.9038	-1.3145	4.5893	6.0119	5.9038	1.3145	3.6091	2.2946	0.4358	0.0655	0.2638	0.0590	89.4 (5 mM) 93.1 (10 mM)
3-AB	-5.7919	-1.4035	4.3884	8.0848	5.7919	1.4035	3.5977	2.1942	0.4557	0.0712	0.2785	0.0643	93.0 (5 mM) 94.5 (10 mM)

[a] values obtained from Ref. [30].

The global hardness η defined as:

$$\eta = \frac{I - A}{2} \tag{9}$$

The softness (σ) of the inhibitor molecule is simply reverse of the global hardness: $\sigma = 1/\eta$. When the inhibitor molecule and metallic iron surface are brought together, electron flow will occur from the inhibitor molecule to the iron atoms until and unless the chemical potentials become equal. It can be presumed, electron transfer in fraction from the inhibitor to the metal surface is calculated by the following equation:[56]

$$\Delta N = \frac{\chi_{Fe} - \chi_{inh}}{2(\eta_{Fe} + \eta_{inh})} \tag{10}$$

OPTIMIZED GEOMETRY

HOMO ORBITALS

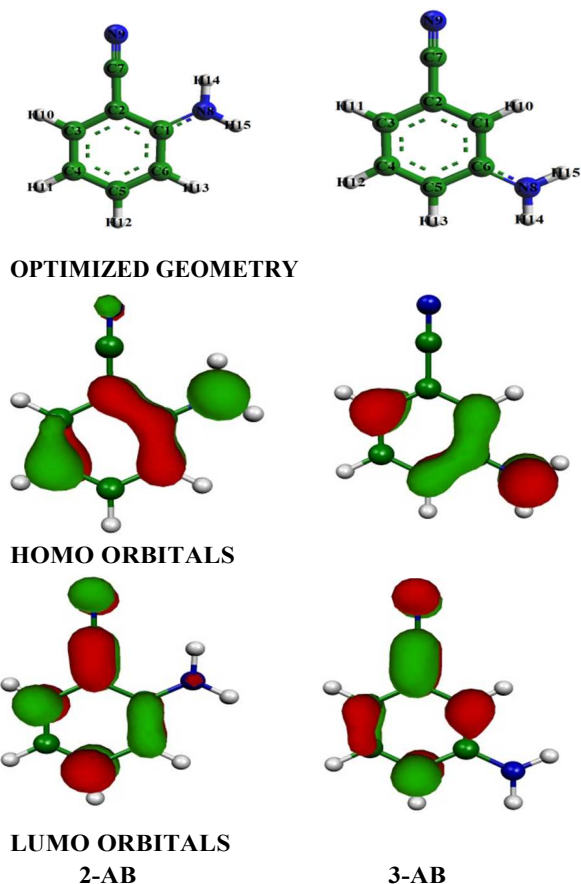**LUMO ORBITALS**

       2-AB   **3-AB**

Fig. 2 The optimized geometry: HOMO and LUMO orbitals of 2-AB and 3-AB at the B3LYP/ SV(P), SV/J level of basis set for neutral species in aqueous phase.

From the literature, it can be seen that fraction of electron transferred is calculated by taking a theoretical value for the absolute electronegativity of iron is χ_{Fe}= 7eV [56,57,58] and global hardness of $\eta_{Fe} = 0$, since $I = A$ for metallic bulk atoms.[59] Actually, the usage of χ_{Fe} value of 7eV is not conceptually correct as it is only associated with the free electron gas Fermi energy of iron where electron-electron interaction is not taken into the consideration.[41,60,61,62] For this reason, now-a-days researchers have used work function (ϕ) of a metal surface, which is more appropriate measure of its electronegativity.[41,61,62] Therefore, ΔN value calculation is more appropriate by the usage of work function (ϕ). For this reason, to measure the ΔN value more specifically χ_{Fe} is replaced by ϕ in the eq. 10. Thus, eq. 10 is written as follows

$$\Delta N = \frac{\phi - \chi_{inh}}{2(\eta_{Fe} + \eta_{inh})} \tag{11}$$

From DFT calculations, the obtained ϕ values are 3.91 eV, 4.82 eV and 3.88 eV for Fe (100), (110) and (111) surfaces, respectively.[41,61] Electron transfer will happen from molecule to metal surface if $\Delta N > 0$ and vice versa if $\Delta N < 0$.[60] According to Elnga *et al*., electron-donating ability of the molecule increases if $\Delta N < 3.6$.[52] From Table 2, it is seen that ΔN values are positive and less than 3.6 for the interaction between the inhibitor molecules and three Fe planes, it is also observed within the limit of 3.6 for ΔN it increases in the following order: 2-AB < 3-AB. This result indicates that 3-AB molecule donates its electron in higher fraction than that of 2-AB and this outcomes correlate strongly with the experimentally obtained inhibition efficiency.

Adsorption of inhibitor molecule on the metallic surface also allied with the softness (σ) of the inhibitor molecule. In this donor accepter chemistry, the metals are considered as soft acid and the inhibitors as soft base.[28] Thus, soft-soft interaction is the controlling factor for the adsorption of inhibitor molecules. It can be seen from Table 2, that the calculated values of softness follows the trend: 3-AB > 2-AB, which further supports the better adsorption proficiency of 3-AB on the metal surface.

3.3. Active sites

Inhibitor molecules are in general adsorbed on the metallic surface by the donor acceptor (D-A) type interaction between the inhibitor molecule and the concerned metallic surface. Therefore, it is essential to examine which corresponding active sites are responsible for this. Generally more is the negatively charge on the heteroatoms, more it can participate on the D-A type interactions.[63] But it is also important to consider the situation from where the inhibitor molecules is going to receive certain amount of charges at some centres and reverting back for donating considerable amount of charges through consecutive centres.[59] This can be easily achieved by evaluating of Fukui indices for each an individual atom. It provides local reactivity as well as nucleophilic and electrophilic nature of the molecule.[64] Nucleophilic and electrophilic attacks are mainly controlled by the maximum threshold values of f_k^+ and f_k^-. f_k^+ measures changes in electron density when the molecule accept extra

Table 3 Calculated Fukui functions for the two inhibitor molecules

Atoms	2-AB		3-AB	
	f_k^+	f_k^-	f_k^+	f_k^-
C (1)	0.057	0.065	0.097	0.088
C (2)	0.073	0.073	0.086	0.047
C (3)	0.098	0.061	0.072	0.111
C (4)	0.056	0.117	0.067	0.055
C (5)	0.119	0.053	0.108	0.083
C (6)	0.079	0.087	0.047	0.069
C (7)	0.100	0.034	0.114	0.023
N (8)	0.046	0.168	0.035	0.190
N (9)	0.159	0.086	0.174	0.056

Table 4 DFT (ORCA) derived Mulliken atomic charges of the two studied inhibitor molecules in neutral form

Atoms	2-AB	3-AB
C (1)	0.178722	-0.183255
C (2)	-0.016208	0.008558
C (3)	0.087793	-0.096872
C (4)	-0.090777	-0.063501
C (5)	-0.040834	-0.144072
C (6)	-0.177634	0.221722
C (7)	0.201914	0.268564
N (8)	-0.385521	-0.429527
N (9)	-0.456172	-0.443178

electrons whereas f_k^- measure electron density changes when molecule losses electrons.

The calculated Fukui indices of the two studied inhibitor molecules are tabulated in Table 3. It can be seen from Table 3 that in 2-AB molecule C(1), C(2), C(3), C(5), C(6), C(7) and N(9) atoms are the more susceptible sites for nucleophilic attack (electron acceptance) as those atoms possess higher charge densities. On the other hand C(1), C(2), C(3), C(4), C(6), N(8) and N(9) atoms are mainly participated in electrophilic attack (donation of electrons). Therefore, it can be concluded from these results that all the individual atoms will be participated in the D-A type interaction on the iron surface. However in 3-AB, after the shifting of –NH₂ group ortho position to meta position, the distribution of active sites and their values are nearly similar. Here, C(1), C(2), C(3), C(4), C(5), C(7) and N(9) atoms are the favorable sites for electrons acceptance while C(1), C(3), C(5), C(6) and N(8) atoms will be responsible for electron donation.

In view of above discussion, it can be concluded that both the molecules have good many number of active centres for their D-A type interaction with the concerned iron surfaces. It can also be seen that the distribution of electronic density in the HOMO and LUMO orbitals of the two inhibitor molecules are in well agreement with the calculated Fukui indices. Thus, the outcomes support the same reactive zones for nucleophilic and electrophilic attack on the iron surface.

3.4. Molecular structure consideration

According to the wet chemical experimentation (potentiodynamic polarization, EIS) corrosion inhibition efficiencies with varying concentration followed the order 3-AB > 2-AB. Fukui indices analysis suggests that both the molecules have almost same active sites for their D-A accepter type interaction on the iron surface. Then the obvious question is coming how 3-AB showing higher inhibition efficiency in comparison to 2-AB. This question can be successfully explained by their molecular configuration. From the geometry optimized structure of 2-AB it can be seen that the distance between the N atom in -C≡N group and H atom in amine-NH₂ group is 2.960 Å. Therefore, intramolecular H-bonding between these two atoms can easily occur. However in 3-AB, intermolecular hydrogen bonding between the molecules will occur (Fig. 3) as the -NH₂ group is situated meta position with respect to the -C≡N group. Possibly these two different types of H-bonding creates major differences in their inhibition efficiencies.

Intramolecular hydrogen bonding in 2-AB prevents their chain propagation between the molecules and thereby molecule behave as a single unit whereas in 3-AB chain propagation will easily occur through the intermolecular hydrogen bonding. It is well known that higher the surface coverage by the inhibitor molecule higher is the inhibition efficiency. Therefore due to the intermolecular H-bonding, 3-AB definitely provides larger blocking area on the steel surface and prevents possible acidic attack on it. Thus higher inhibition efficiency is expected by the 3-AB molecule and it is also observed accordingly in the wet chemical experimentation.
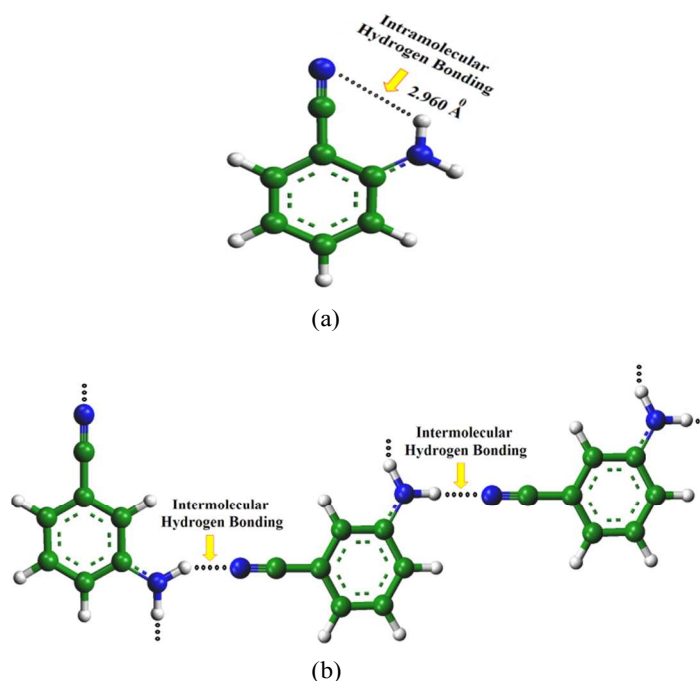

(a)

(b)

Fig. 3 Two different types of Hydrogen Bonding: (a) Intramolecular Hydrogen Bonding (2-AB); (b) Intermolecular Hydrogen Bonding (3-AB).

The above mentioned explanation is true in case of chemisorption. As it is well known that molecules adsorb on the metallic surface by chemisorption and physisorption. Thus obvious question is coming how molecules behave in physisorption. This explanation can be

explained in terms of Mulliken atomic charges of the neutral form of inhibitor molecules. It is found from Mulliken atomic charges (*vide* Table 4) that N atoms in the aminobenzonitrile ring have highest negative charges among the other atoms. Hence, highest probability of lowest energy upon their protonation. After the protonation in the acidic solution both the molecule behaves as single unit as because no way to form intramolecular or intermolecular hydrogen bonding. Thus in the protonated form both the molecule adsorb on the iron surface as a single unit. As a result the differences in inhibition efficiency between these two molecules are coming from the chemisorption process. It is already stated intermolecular hydrogen bonding favours higher surface coverage on the iron surface during the adsorption process, higher inhibition efficiency is expected and it is observed accordingly in the wet chemical analysis. Therefore it can be concluded from this explanation that intermolecular hydrogen bonding in 3-AB plays a significant role for its higher inhibition efficiency.

3.5. Quantum chemical calculations of protonated form of inhibitor molecules

Presence of heteroatoms in the aminobenzonitrile molecule suggests their high tendency towards protonation in the acidic medium. Therefore, it is obvious to investigate the protonated forms of inhibitor molecule. It is apparent from Fig. 1 that in the aminobenzonitrile ring more than one N atoms is present. Thus, we have to decide which atom posses lowest energy upon their protonation. In order to find it out, geometry optimization of two possible structures are carried out and it is observed that most favourable one with lowest energy upon their protonation is the N atoms which carries highest negative charges on it.[65,66] From Table 4 it is seen that, N9 atom in both the inhibitors posses highest negative charges. Thus, in this present investigation N9 atom is protonated. The optimized geometric configurations, HOMO and LUMO orbitals of the molecules (2-AB and 3-AB) are shown in Fig. 4 and their bond angle, bond lengths, mulliken atomic charges are presented in Table 5 and 6. From Table 5 and 6 it can be seen that after protonation there is a significant difference in their bond length, bond angle and mulliken atomic charges. Thus, the reactivity of the inhibitor molecules in their protonated forms should be considered. From Table 7 it can be seen that E_{HOMO} values for both the inhibitors are shifted towards the more negative value in comparison to the E_{HOMO} values of neutral form. It signifies that in protonated form, electron donation capability of the inhibitor molecules is decreased and it is also expected as after protonation inhibitor molecules are not capable enough to donate their electrons to the metallic surfaces. This fact is further confirmed by the fraction of electron transferred from the inhibitors to the metallic surface (ΔN). Inspection of Table 7 shows that all the values of ΔN for Fe (1 0 0) and Fe (1 1 1) surface is negative whereas for Fe (1 1 0) plane values are positive but relatively very small. On the other hand, if we look at the E_{LUMO} values it can be seen that E_{LUMO} values is also shifted towards the more negative values than its neutral form, it pointing out electron acceptance capability in protonated from is increased and it can be also seen that electron acceptance capability of 3-AB molecule is higher than the 2-AB molecule. It is further counter supported by the electronegativity values of the two inhibitors. Comparison of electronegativity values of the two forms of inhibitors molecules reflects that electronegativity values in the protonated form of inhibitor molecules is much higher than that of the neutral form. It reflects electron attraction capability from the metal surface is increased by the protonated form of inhibitor molecules. Therefore, after a complete analysis of the both the form of inhibitors molecules it can be concluded that the neutral form of inhibitors molecule have

higher tendency to donates their electrons and protonated form of inhibitors molecules have superior tendency to accept electrons. Now, it is clear from the above mention discussion that a more complete analysis of reactivity is obtained from both the form of inhibitor molecules.

Table 5 Bond length (Å) and bond angle (°) of the optimized protonated form of inhibitor molecules

Geometry parameters	2-AB	3-AB
Bond length		
C1—C2	1.4372	1.4108
C2—C3	1.4294	1.4121
C3—C4	1.3769	1.3951
C4—C5	1.4176	1.3955
C5—C6	1.3827	1.4166
Bond angle		
C1—C2—C3	121.42	122.67
C2—C3—C4	119.90	117.28
C3—C4—C5	119.10	120.99
C4—C5—C6	121.94	121.75
C5—C6—C1	121.04	118.11

OPTIMIZED GEOMETRY

HOMO ORBITALS　　　　　**LUMO ORBITALS**
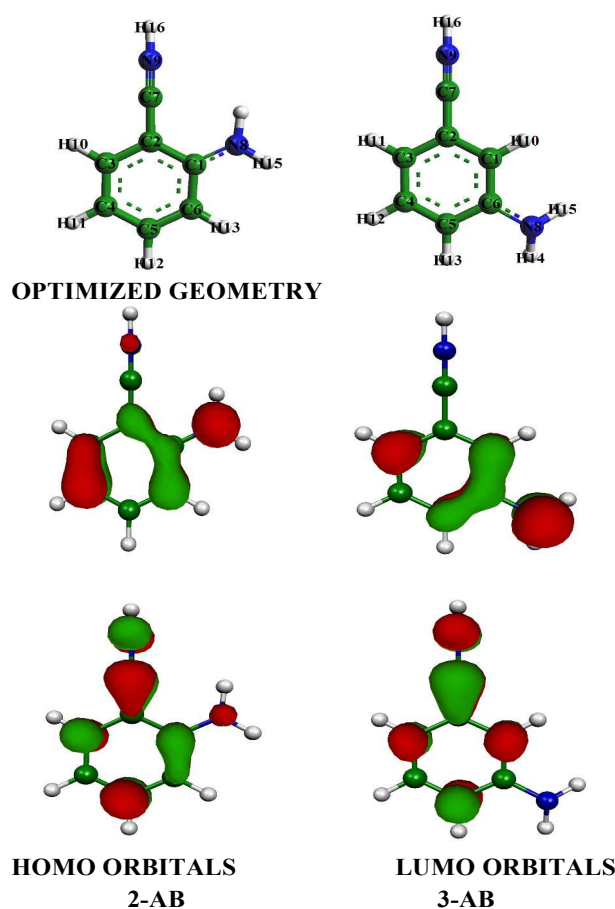**2-AB**　　　　　　　　　　　　**3-AB**

Fig. 4 The optimized geometry: HOMO and LUMO orbitals of 2-AB and 3-AB at the B3LYP/ SV(P), SV/J level of basis set for protonated species in aqueous phase.

Table 6 DFT (ORCA) derived Mulliken atomic charges of the two studied inhibitor molecules in protonated form

Atoms	2-AB	3-AB
C (1)	0.197506	-0.128874
C (2)	-0.070681	-0.048813
C (3)	-0.046695	-0.051847
C (4)	-0.078492	-0.056618
C (5)	-0.019974	-0.098080
C (6)	-0.157599	0.164597
C (7)	0.676637	0.745164
N (8)	-0.336000	-0.390005
N (9)	-0.381233	-0.338468

Table 7 Calculated quantum chemical parameters of the studied inhibitors in protonated form

| Inhibitors	E_{HOMO} (eV)	E_{LUMO} (eV)	ΔE (eV)	μ (Debye)	$I = -E_{HOMO}$	$A = -E_{LUMO}$	χ (eV)	η (eV)	σ (eV^{-1})	ΔN_{100}	ΔN_{110}	ΔN_{111}	Inhibition efficiency
2-AB	-6.4759	-2.4088	4.0671	7.3572	6.4759	2.4088	4.4423	2.0335	0.4917	-0.1309	0.0928	-0.1382	89.4 (5 mM); 93.1 (10 mM)
3-AB	-6.3772	-2.6499	3.7273	7.2501	6.3772	2.6499	4.5135	1.8636	0.5365	-0.1619	0.0822	-0.1699	93.0 (5 mM); 94.5 (10 mM)

3.6. Molecular dynamics simulation

Molecular dynamics (MD) simulation recently considered as a modern tool to study the adsorption behavior of the inhibitor molecules on the concerned metallic surfaces. Recently Obot *et al*, Xia *et al*, Tang *et al*, Musa *et al* and many other scientists are working on it to understand the adsorption process of the corrosion inhibitors.[28,29,41,57] Thus, in order to get more suitable and adorable adsorption configuration of the studied inhibitors molecules, MD simulation is carried out in this present investigation.

The first step of this investigation is the geometry optimization of the studied inhibitors, solvent molecules (H_2O) and corrosive hydronium ions (H_3O^+). Geometry optimization is carried out by employing a 'smart' algorithm, started with a steepest descent path then followed the conjugate gradient path and finally ended with the Newton's method.[40] During the course of the geometry optimization process atomic coordinates are adjusted based on COMPASS forcefield[47] until and unless the total energy of the individual structure reaches the minimum energy, afterwards a simulation box is created by the all concerned species. In this context, simulation will be completed when the temperature and energy of the system reaches equilibrium. It can be seen from Fig. 5 and 6 that at the middle of the simulation process the system tends towards equilibrium. After the system reaches equilibrium $E_{interaction}$ and $E_{binding}$ energy of the surface adsorbed inhibitor molecules are calculated according to eqn. 4 and 5 respectively. The obtained $E_{interaction}$ and $E_{binding}$ values are tabulated in Table 8. The best adorable adsorption configurations of the inhibitor molecules over the Fe (1 1 0) surface are depicted in Fig. 7. It can be seen from this figures that inhibitor molecules adsorb almost flat orientation with respect to the iron surface. This flat orientation

can be explained in terms of chemical bond formation between the inhibitors and iron surface.

Generally, the bond distance within 3.5Å indicates the formation of strong chemical bond between the atoms and the bond distance above 3.5Å signifies interaction between the atoms are of Van der Waals type.[67,68] Fig. 7 (a) and (c) shows the shortest bond distances between the heteroatoms of the inhibitors and Fe atoms. The measured shortest bond distances for the two inhibitors are as follows: 2-AB − Fe interaction: (Fe-N8 = 3.072Å, Fe-N9 = 3.064Å); 3-AB − Fe interaction: (Fe-N8 = 3.331Å, Fe-N9 = 3.262Å). From the above mentioned values it is seen that all the shortest bond distances are within the range of 3.5Å, it indicates that a chemical bond is formed between the inhibitor molecule and Fe surface atom. Hence, a chemical adsorption will occur on Fe surfaces. Thus, it is further confirmed from the MD simulations that adsorption of the inhibitor molecules on the metallic surfaces mainly occurred by the chemical adsorption phenomenon.

Additionally, it could be seen (*vide* Table 8) that the calculated interaction energy values of the adsorption systems at 298 K are -347.30 and -361.88 kJ/mol respectively. These larger negative values of interaction energies can be ascribed due to the strong interaction between the studied inhibitors molecules and iron surfaces. Thus calculated interaction energy values reveal that 3-AB molecule adsorb on the iron surface more spontaneously than that of 2-AB. Moreover, the adsorption ability of the molecule on the iron surface can also be measured from the binding energy values. Higher is the binding energy, more will be the adsorption. Thus, it can be seen from the interaction energy as well as from binding energy values that the adsorption ability of the inhibitors molecules on the iron surface at 298 K follows the order: 3-AB > 2-AB. These outcomes are in good agreement with the results obtained from wet chemical experimentation.

(a)   (b)
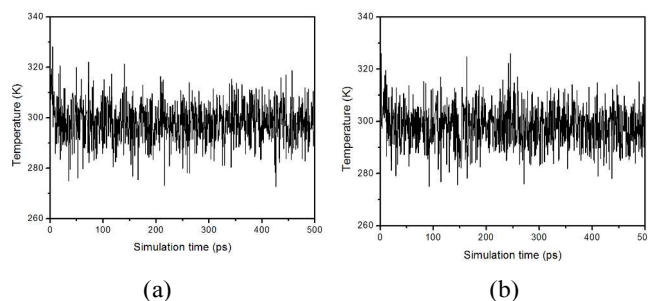
Fig. 5 Temperature equilibrium curve obtained from MD simulation for (a) 2-AB and (b) 3-AB at 298 K.
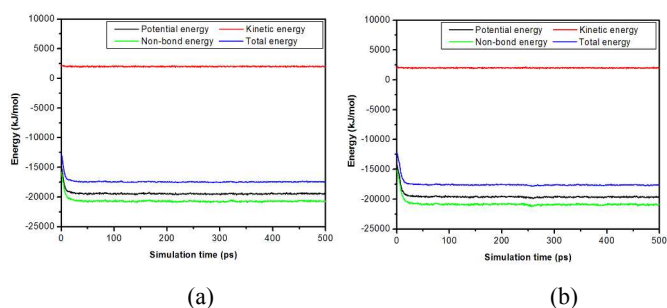
Fig. 6 Energy fluctuation curves obtained from MD simulation for (a) 2-AB and (b) 3-AB at 298K.

Table 8 Output obtained from MD simulation for adsorption of inhibitors on Fe (1 1 0) surface

Systems	$E_{interaction}$ (kJ/mol)		$E_{binding}$ (kJ/mol)	
	298K	328K	298K	328K
Fe + 2-AB	−347.30	−301.27	347.30	301.27
Fe + 3-AB	−361.88	−333.75	361.88	333.75
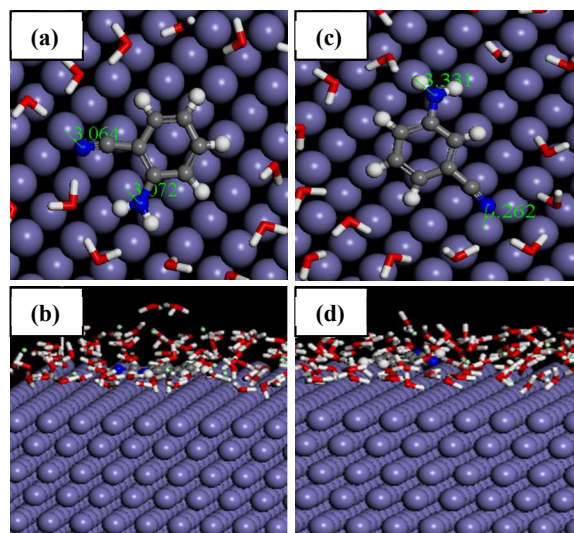
Fig. 7 Equilibrium adsorption configurations of inhibitors 2-AB (a and b) and 3-AB (c and d) on Fe (1 1 0) surface at 298 K obtained from MD simulations. Top: top view, Bottom: side view.

In order to investigate the effect of temperature on the corrosion inhibition efficiencies of the inhibitors molecules, in this present investigation MD simulations are also carried out at 328 K. Here, we have increased the simulation temperature from 298 K to 328 K. The obtained temperature equilibrium curves, energy fluctuation curves and best adorable adsorption configuration of the inhibitors over Fe (1 1 0) surface are depicted in Fig. S1, S2 and S3 respectively. The results reflects that (*vide* Table 8) with increasing temperature adsorption energy and binding energy values of the inhibitor molecules on the Fe (1 1 0) surface are decreased and we are well familiar that if interaction energy and binding energy decreased lower inhibition efficiency is expected. From, wet chemical analysis it is seen that when temperature increases from 298K to 328K inhibition efficiency of the inhibitors molecules is decreased. Therefore, MD simulation results corroborated with the experimental findings. As a result, MD simulations can also be used to predict the molecular behavior of the inhibitor molecules in the higher temperature range. Thus in conclusion it can be said that these results are in good agreement with the results obtained from wet chemical experimentation as well as from quantum chemical calculations.

4. Conclusion

A combined theoretical analysis (classical and quantum chemical approach) is performed to study the corrosion inhibition performance of two aminobenzonitrile compounds on the steel surface. It is evident from this investigation that only theoretical studies can provide a complete insightfulness into the chemical reactivity of the studied inhibitor molecule. It also offers atomic level investigation of the experimental findings. The followings outcomes can be concluded from this study:

(i) Quantum chemical calculation reveals that electron donation and electron acceptance capability of the studied inhibitors follows the order 3-AB > 2-AB, which is in well accordance with the results obtained from previously performed experimental findings.
(ii) Active sites of the studied inhibitors molecules are also thoroughly investigated by Fukui indices. Fukui indices describe in detail which particular atoms are mainly participated for the electron donation and acceptance process between the inhibitors and Fe surface.
(iii) Molecular structure consideration has suggested that two different kinds of hydrogen boning are formed for studied inhibitor molecules. In 2-AB, intramoleular hydrogen bonding is formed where as intermolecular hydrogen bonding is present in 3-AB. These two different types of hydrogen bonding are responsible for their different inhibition efficiencies.
(iv) MD simulation reveals that the all the shortest bond distances between the heteroatoms of the inhibitors and Fe atoms are lying within a range of 3.5Å. It suggests, a chemical bond is formed between the inhibitors and Fe atoms. Owing to chemical adsorption, aminobenzonitrile inhibitors adsorb on the steel surfaces in the parallel orientation. An interaction energy and binding energy value of the two studied inhibitors also obeys the order of 3-AB > 2-AB. These outcomes are in well accordance with the experimental findings.
In conclusion, the above mentioned results obtained from two different domains starting from density functional theory (based on quantum chemistry) to MD simulation (based on classical physics) are in fine agreement with the previously obtained experimental results. It can be concluded that DFT along with MD simulation may be a very powerful tool for the rational designing of several promising corrosion inhibitors and in prediction of their inhibition efficiency well in advance.

Acknowledgements

Notes and references

[a]Surface Engineering & Tribology Group, CSIR-Central Mechanical Engineering Research Institute, Mahatma Gandhi Avenue, Durgapur 713209, West Bengal, India.

E-mail: pr_banerjee@cmeri.res.in; Fax: +91-343-2546 745; Tel: +91-343-6452220

[b]Academy of Scientific & Innovative Research at CSIR-CMERI, Durgapur 713209, India

†Electronic Supplementary Information (ESI) available: [Temperature equilibrium curves, energy fluctuation curves and Equilibrium adsorption configurations of the studied inhibitors (at 328 K) are included in the supplementary information]. See DOI: 10.1039/b000000x/

[1] K. Mallaiya, R. Subramaniam, S. S. Srikandan, S. Gowri, N. Rajasekaran and A. Selvaraj, Electrochim. Acta, 2011, 56, 3857.

[2] N. A. Negma, N. G. Kandile, E. A. Badr and M. A. Mohammed, Corros. Sci., 2012, 65, 94.

[3] B. Y. Liu, Z. Liu, G. C. Han and Y. H. Li, Thin solid flims, 2011, 519, 7836.

[4] S. A. A. El-Maksoud and A. S. Fouda, Mater. Chem. Phys., 2005, 93, 84.

[5] H. Keles, M. Keles, I. Dehri and O. Serindag, Mater. Chem. Phys., 2008, 112, 173.

[6] M. A. Hegazy, A. M. Hasan, M. M. Emara, M. F. Bakr and A. H. Youssef, Corros. Sci., 2012, 65, 67.

[7] M. Lagrenee, B. Mernari, M. Bouanis, M. Traisnel and F. Bentiss, Corros. Sci., 2002, 44, 573.

[8] M. Behpour, S. M. Ghoreishi, N. Mohammadi, N. Soltani and M. Salavati-Niasari, Corros. Sci., 2010, 52, 4046.

[9] M. G. Hosseini, M. Ehteshamzadeh and T. Shahrabi, Electrochim. Acta, 2007, 52, 3680.

[10] A. Aytaç, Ü. Özmen and M. Kabasakaloˇlu, Mater. Chem. Phys., 2005, 89, 176.

[11] K. R. Ansari, M. A. Quraishi and A. Singh, Corros. Sci., 2014, 79, 5.

[12] R. Solmaz, E. A. Sahin, A. Döner and G. Kardas, Corros. Sci., 2011, 53, 3231.

[13] O. K. Abiola and N. C. Oforka, Mater. Chem. Phys., 2004, 83, 315.

[14] M. G. V. Satyanarayana, V. Himabindu, Y. Kalpana, M. R. Kumar and K. Kumar, J. Mol. Struc. (Theochem), 2009, 912, 113.

[15] T. H. Muster, A. E. Hughes, S. A. Furman, T. Harvey, N. Sherman, S. Hardin, P. Corrigan, D. Lau, F. H. Scholes, P. A. White, M. Glenn, J. Mardel, S. J. Garcia and J. M. C. Mol, Electrochim. Acta., 2009, 54, 3402.

[16] S. Sun, Y. Geng, L. Tian, S. Chen, Y. Yan and S. Hu, Corros. Sci., 2012, 63, 140.

[17] M. Mousavi, M. Mohammadalizadeh and A. Khosravan, Corros. Sci., 2011, 53, 3086.

[18] J. M. Roque, T. Pandiyan, J. Cruz and E. Garcı´a-Ochoa, Corros. Sci., 2008, 50, 614.

[19] E. Jamalizadeh, S. M. A. Hosseini and A. H. Jafari, Corros. Sci., 2009, 51, 1428.

[20] G. Gece and S. Bilgiç, Corros. Sci., 2010, 52, 3435.

[21] S. K. Saha, A. Hens, A. R. Chowdhury, A. K. Lohar, N. C. Murmu and P. Banerjee, Can. Chem. Trans., 2014, 2, 489.

[22] S. K. Saha, P. Ghosh, A. Hens, N. C. Murmu and P. Banerjee, Physica E, 2015, 66, 332.

[23] S. K. Saha, A. Dutta, P. Ghosh, D. Sukul and P. Banerjee, Phys. Chem. Chem. Phys., 2015, 17, 5679.

[24] A. Kokalj, Electrochim. Acta., 2010, 56, 745.

[25] N. Kovačević and A. Kokalj, Corros. Sci., 2011, 53, 909.

[26] E. E. Ebenso, M. M. Kabanda, L. C. Murulana, A. K. Singh and S. K. Shukla, Ind. Eng. Chem. Res., 2012, 51, 12940.

[27] Sudheer and M. A. Quraishi, Corros.Sci., 2013, 70, 161.

[28] I. B. Obot and Z. M. Gasem, Corros.Sci., 2014, 83, 359.

[29] S. Xia, M. Qiu, L. Yu, F. Liu and H. Zhao, Corros. Sci., 2008, 50, 2021.

[30] G. Sığırcık, T. Tüken and M. Erbil, Appl. Sur. Sci., 2015, 324, 232.

[31] F. Neese, An Ab initio, DFT and Semiempirical SCF-MO Package, Version 2.7.0; Max Planck Institute for Bioinorganic Chemistry, Mulheim an der Ruhr, Germany, Jan (2012).

[32] D. A. Becke, J. Chem. Phys., 1986, 84, 4524.

[33] D. A. Becke, J. Chem. Phys., 1993, 98, 5648.

[34] C. Lee, W. Yang and G. R. Parr, Phys. Rev. B., 1988, 37, 785.

[35] P. Banerjee, A. Company, T. Weyhermuller, E. Bill and C. R. Hess, Inorg. Chem., 2009, 48, 2944.

[36] P. Banerjee, S. Sproules, T. Weyhermuller, S. D. George and K. Wieghardt, Inorg. Chem., 2009, 48, 5829.

[37] S. Joy, T. Krämer, N. D. Paul, P. Banerjee, J. E. McGrady and S. Goswami, Inorg. Chem., 2011, 50, 9993.

[38] A. Schafer, C. Huber and R. Ahlrichs, J. Chem. Phys., 1994, 100, 5829.

[39] A. Schafer, H. Horn and R. Ahlrichs, J. Chem. Phys., 1992, 97, 2571.

[40] Materials Studio 6.1 Manual (Accelrys, Inc., San Diego, CA, 2007).

[41] Z. Cao, Y. Tang, H. Cang, J. Xu, G. Lu and W. Jing, Corros. Sci., 2014, 83, 292.

[42] J. A. Ciezak and S. F. Trevino, J. Phys. Chem. A., 2006, 110, 5149.

[43] R. G. Parr and W. Yang, J. Am. Chem. Soc., 1984, 106, 4049.

[44] F. D. Proft, J. M. L. Martin and P. Geerlings, Chem. Phys. Lett., 1996, 256, 400.

[45] R. R. Contreras, P. Fuentealba, M. Galvan and P. Perez, Chem. Phys. Lett., 1999, 304, 405.

[46] F. L. Hirshfeld, Theor. Chem. Acc., 1977, 44, 129.

[47] H. Sun, J. Phys. Chem. B., 1998, 102, 7338.

[48] P. Ghosh, B. G. Roy, S. K. Mukhopadhyay and P. Banerjee, RSC Adv., 2015, 5, 27387.

[49] D. Özkır, K. Kayakırılmaz, E. Bayol, A. A. Gürten and F. Kandemirli, Corros. Sci., 2012, 56, 143.

[50] N. O. Obi-Egbedi and I. B. Obot, Corros. Sci., 2011, 53, 263.

[51] K. F. Khaled, Appl. Surf. Sci., 2008, 255, 1811.

[52] M. K. Awad, M. R. Mustafa and M. M. Abo Elnga, J. Mol. Struc. (Theochem), 2010, 959, 66.

[53] M. Sahin, G. Gece, F. Karci and S. Bilgic, J. Appl. Electrochem., 2008, 38, 809.

[54] M. A. Quraishi and R. Sardar, J. Appl. Electrochem., 2003, 33, 1163.

[55] I. Lukovits, E. Kalman and F. Zucchi, Corrosion 2001, 57, 3.

[56] S. Martinez, Mater. Chem. Phys., 2002, 77, 97.

[57] A. Y. Musa, R. T. T. Jalgham and A. B. Mohamad, *Corros. Sci.*, 2012, **56**, 176.

[58] A. Y. Musa, A. A. H. Kadhum, A. B. Mohamad, M. S. Takriff, *Mater. Chem. Phys.*, 2011, **129**, 660.

[59] H. Shokry, *J. Mol. Struc.,* 2014, **1060**, 80.

[60] N. Kovačević and A. Kokalj, *J. Phys. Chem. C*, 2011, **115**, 24189.

[61] A. Kokalj, *Chem. Phys.*, 2012, **393**, 1.

[62] I. B. Obot, D. D. Macdonald, Z. M. Gasem, *Corros. Sci.*, doi: 10.1016/j.corsci.2015.01.037

[63] G. Breket, E. Hur and C. Ogretir, *J. Mol. Struct. (Theochem)*, 2002, **578**, 79.

[64] M. A. Hegazy, A. M. Badawi, S. S. Abd El Rehim, W. M. Kamel, *Corros. Sci.,* 2013, **69,** 110.

[65] M. M. Kabanda, L. C. Murulana, M. Ozcan, F. Karadag, I. Dehri, I. B. Obot and E. E. Ebenso, *Int. J. Electrochem. Sci.*, 2012, **7**, 5035.

[66] N. O. Obi-Egbedi, I. B. Obot, M. I. El-Khaiary, S. A. Umoren and E. E. Ebenso, *Int. J. Electrochem. Sci.*, 2012, **7,** 5649.

[67] W. Y. Shi, C. Ding, J. L. Yan, X. Y. Han, Z. M. Lv, W. Lei, M. Z. Xia and F. Y. Wang, Desalination 2012, **29**, 18.

[68] J. P. Zeng, J. Y. Zhang, X. D. Gong, *Comput. Theor. Chem.*, 2011, **963**, 110.